ESC European Society of Cardiology

European Heart Journal - Imaging Methods and Practice (2024) **2**, qyae100
https://doi.org/10.1093/ehjimp/qyae100

ORIGINAL ARTICLE

Assessing left atrial dysfunction in cardiac amyloidosis using LA–LV strain slope

Fredrik Edbom [1,*], Per Lindqvist [1], Urban Wiklund [2], Björn Pilebro[3], Intissar Anan[4], Frank A. Flachskampf [5], and Sandra Arvidsson[1]

[1]Department of Diagnostics and Intervention, Clinical Physiology, Umeå University, Universitetstorget 4, 90187 Umeå, Sweden
[2]Department of Diagnostics and Intervention, Biomedical Engineering and Radiation Physics, Umeå University, Umeå, Sweden
[3]Department of Public Health and Clinical Medicine, Cardiology, Umeå University, Umeå, Sweden
[4]Department of Public Health and Clinical Medicine, Medicine, Umeå University, Umeå, Sweden
[5]Department of Medical Sciences, Clinical Physiology, Uppsala University, Uppsala, Sweden

Received 13 May 2024; accepted after revision 9 September 2024; online publish-ahead-of-print 26 September 2024

Abstract

Aims

Transthyretin amyloid cardiomyopathy (ATTR-CM) is an infiltrative disease of the myocardium in which extracellular deposits of amyloid cause progressive cardiac impairment. We aimed to evaluate left atrial (LA) deformation and its association with left ventricular (LV) deformation using LA–LV strain loops in patients with ATTR-CM and patients with LV hypertrophy (LVH). We hypothesized that LA strain in ATTR-CM patients is abnormal and more independent of LV strain, compared to LVH patients.

Methods and results

Retrospective study based on echocardiographic data including 30 patients diagnosed with ATTR-CM based on an end-diastolic interventricular septal (IVSd) thickness of ≥14 mm, and 29 patients with LVH (IVSd ≥ 14 mm and no ATTR-CM diagnosis) together with 30 controls. LV global longitudinal strain (LV-GLS) and LA strain, assessed as peak atrial longitudinal strain (PALS), were acquired and plotted to construct LA–LV strain loops and used regression line to determine a LA–LV strain slope. Significantly lower PALS and LA–LV strain slope values were detected in ATTR-CM patients compared to LVH patients ($P = 0.004$ and $P = 0.014$, respectively). A receiver operating characteristic (ROC) curve demonstrated similar area under the curve (AUC) using PALS (AUC 0.72) and LA–LV slope (AUC 0.71), with both resulting in higher values than recorded for LV-GLS (AUC 0.62).

Conclusion

LA deformation demonstrates an independent ability to differentiate ATTR-CM from LVH. Combining LV strain and LA deformation analysis displays the mechanical LA–LV dissociation in ATTR cardiac amyloidosis and potentially unmasks LA amyloid infiltration; this could potentially enable quicker diagnosis and initiation of treatment for ATTR-CM.

Lay summary

Transthyretin amyloidosis is a rare condition where abnormal proteins will misfold and build up deposits in tissue. Affected organs will lose its function with time. If the deposits build up within the heart, the heart walls grow thicker and stiffer and will progressively lead to heart failure and death if left untreated. There is currently no treatment available that can remove these fibrils; however, there are specific treatments available that can slow down this process, but it is important to start this as early as possible.

There are other diseases and conditions that also lead to a thicker heart, for example, long-standing high blood pressure. When investigating patients with suspected heart conditions, thickened heart walls can quite easily be identified by available diagnostic imaging methods. However, it can be very difficult, not to say impossible, to distinguish the underlying cause of this

* Corresponding author. E-mail: fredrik.edbom@umu.se

wall thickening by using traditional techniques. It is very valuable for diagnostic methods to be able and direct suspicion towards correct conditions; this will enable the physician to set correct diagnosis and treatment plan.

We wanted to test new echocardiographic methods that incorporate both the function of the atrium and ventricle of the heart. We could see that there is a difference in heart function between a thick heart with amyloidosis compared to thick hearts due to other conditions.

Graphical Abstract

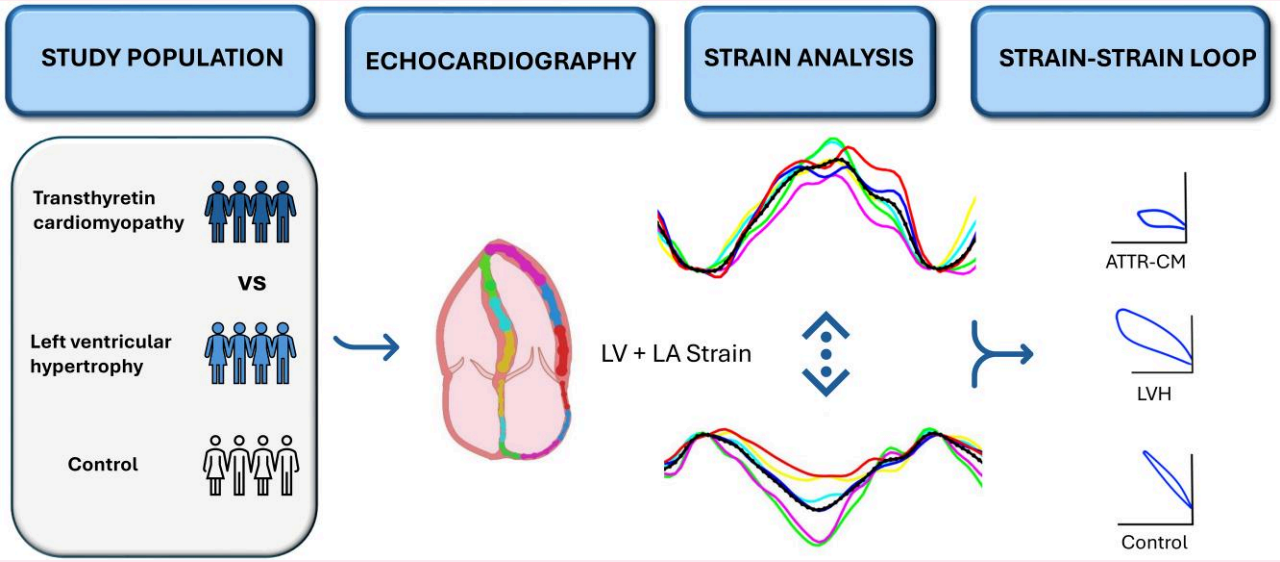

Keywords cardiac amyloidosis • myocardial strain • left atrial function • atrial stiffness • left ventricular hypertrophy • increased myocardial thickness

Introduction

Transthyretin (TTR) amyloidosis cardiomyopathy (ATTR-CM) is a rare, infiltrative disorder caused by misfolding of the TTR protein. This misfolding results in the accumulation of which form protein fragments, forming insoluble fibrils in various tissues and organs including the space around cardiomyocytes. This deposition of amyloid fibrils progressively cause thickening and stiffening of the heart walls, leading to heart failure (HF).[1,2] There are other, more common aetiologies causing increased myocardial thickness, of which hypertension is the most frequent. It is important to distinguish between these two entities at an early stage since they present different pathophysiologies, and treatment should be chosen accordingly.[3] Transthyretin amyloidosis together with immunoglobulin light-chain amyloidosis are the most common types causing cardiac amyloidosis (CA).

There are two main subgroups of ATTR: the hereditary type (ATTRv) and the acquired wild type (ATTRwt).[1,4] Hereditary ATTR and ATTRwt present similar cardiac manifestations, although ATTRwt is more likely to cause cardiac infiltration with a reported incidence increasing with age.[5]

Heart failure is a common consequence of CA.[6] Cardiac amyloid deposits are often detected first during post-mortem, suggesting a significant under-diagnosis of ATTR-CM.[7] Although the left ventricular (LV) myocardium is the most obvious site of amyloid infiltration, studies using both post-mortem evaluations[8,9] and imaging methods[10–12] reveal the atrial is also greatly affected. Atrial amyloid infiltration strongly correlates to the high prevalence of atrial fibrillation (AF) in CA patients.[13] Additionally, the left atrium (LA) plays a significant yet possibly under-recognized role as a driver in HF, and consequently atrial failure has become an increasingly popular term to describe atrial dysfunction.[14,15] This demonstrates the importance of assessing the effects of LA amyloid infiltration, a structure often overlooked when evaluating the overall cardiac function.[15]

To fully assess how amyloid deposits affect cardiac function, assessment of LA function in relation to LV function could potentially unmask regional LA functional impairment due to amyloid infiltration.[16]

Transthoracic echocardiography (TTE) is the cornerstone imaging method, routinely used for evaluating cardiac diseases such as HF. As such, TTE is a suitable method to detect signs of CA.[17] Although CA exhibits a distinct echocardiographic appearance in advanced stages of the disease, it is still considerably difficult to distinguish earlier stages of CA from increased myocardial thickness due to other aetiologies, such as systemic hypertension.[17]

Technical advancements in heart imaging have enabled new methods for evaluation of CA for a better understanding of the clinical presentation, differentiation and prognosis of CA. Examples of such methods include myocardial stiffness,[18] myocardial works,[19,20] and strain analysis for LA or RV.[10,21,22]

Previous studies on CA patients have shown significant more impairment of LA strain compared to other aetiologies associated with increased myocardial thickness.[10,21] Detection of impaired LA strain in

ATTR gene carriers prior to manifestation of the disease implies that LA function analyses could be useful for early disease recognition.[23] Additionally, LA echocardiographic function parameters have demonstrated strong prognostic value in regard to HF and mortality.[12] However, few studies have evaluated the significance of assessing LA function in direct relation to LV function in CA patients.

In a recent study presented by Mălăscue *et al.*,[24] the authors introduced a novel approach using echocardiography to derive a strain–strain loop to simultaneously evaluate the LA and LV function during a complete cardiac cycle. Their results indicate that LV function has a significant impact on LA strain, which supports the theory that LA deformation may have a prognostic value in assessing cardiovascular function.

Although CA and LV hypertrophy (LVH) appear similar on TTE, it is the amyloid infiltration which creates the difference in LV performance, which differentiates the pathways of the two conditions. We hypothesize that there is a clear difference in cardiac performance between CA and LVH pathologies, which can be recognized and visualized by combining LA and LV strain analysis. Furthermore, it is established that survival is significantly improved for ATTR-CM patients with early intervention and targeted treatment, such as with tafamidis, in comparison with those without.[25,26] This emphasizes the importance of identifying diagnostic marker that could identify ATTR-CM to facilitate proper treatment with the aim of improving overall prognosis.

The aim of this study was to assess atrial function for recognition of atrial infiltration in ATTR-CM. The method used was TTE imaging and analysis of LA strain. Comparison of LA strain was made between CA patients and those with LVH due to other pathologies. In addition to using standardized strain methods, we also evaluated the novel LA–LV strain loop method (*Figure 1*).

Methods

Study population

We conducted a single-centre retrospective study on echocardiographic examinations and measurements of patients referred to or recruited to Umeå University Hospital between 2004 and 2022. A population with increased myocardial thickness due to hypertension and/or aortic stenosis as well as diagnosed hypertrophic CM (HCM) were included representing LVH. All 30 patients in an existing database were included. A matched number of patients with known ATTR-CM were additionally included. The control group was composed of 30 heart-healthy individuals.

The general inclusion criteria included echocardiographic image of acceptable quality, electrocardiogram demonstrating sinus rhythm on the day of examination to avoid atrial fibrillation, no pacemaker, no severe valve regurgitation or severe mitral stenosis, and no other known amyloidosis other than TTR. Baseline patient information was obtained from the local medical records at Umeå University Hospital.

Patient groups

Included patients had been diagnosed with ATTR-CM following local routine clinical practice. A positive result for ATTR was regarded as grade II or III with 99mTc-labelled 3,3-diphosphono-1,2-propanodicarboxylic acid (DPD) scintigraphy and/or positive fat tissue biopsy. In addition, genetic testing was performed to determine if patients had ATTRv or ATTRwt.

The LVH group comprised of a subset of different cohorts classified at Umeå University Hospital. These included; treated long-standing hypertension, significant aortic stenosis, or hypertrophic cardiomyopathy. Participants in this group had no amyloidosis diagnosis. It was preferred they had undergone a DPD scintigraphy showing negative result for CA; however, this was not set as a requirement for inclusion. Interventricular septal thickness (IVSd) ≥ 14 mm was the echocardiographic inclusion criteria for both patient groups.

Control group

The included control group individuals were initially recruited as part of the Umeå General Population Heart Study.[27] This subgroup contained participants from Umeå, Sweden, aged 41–81 years, none of which had any suspicion of any cardiovascular or systemic disease additional to normal IVSd (≤12 mm). None of the participants in this group used any medication known to influence cardiac function during the time of recruitment. However, SBP > 150 mmHg was accepted at the time of entry for participants in the healthy control group because of the wide age span within the group (41–81 years of age).

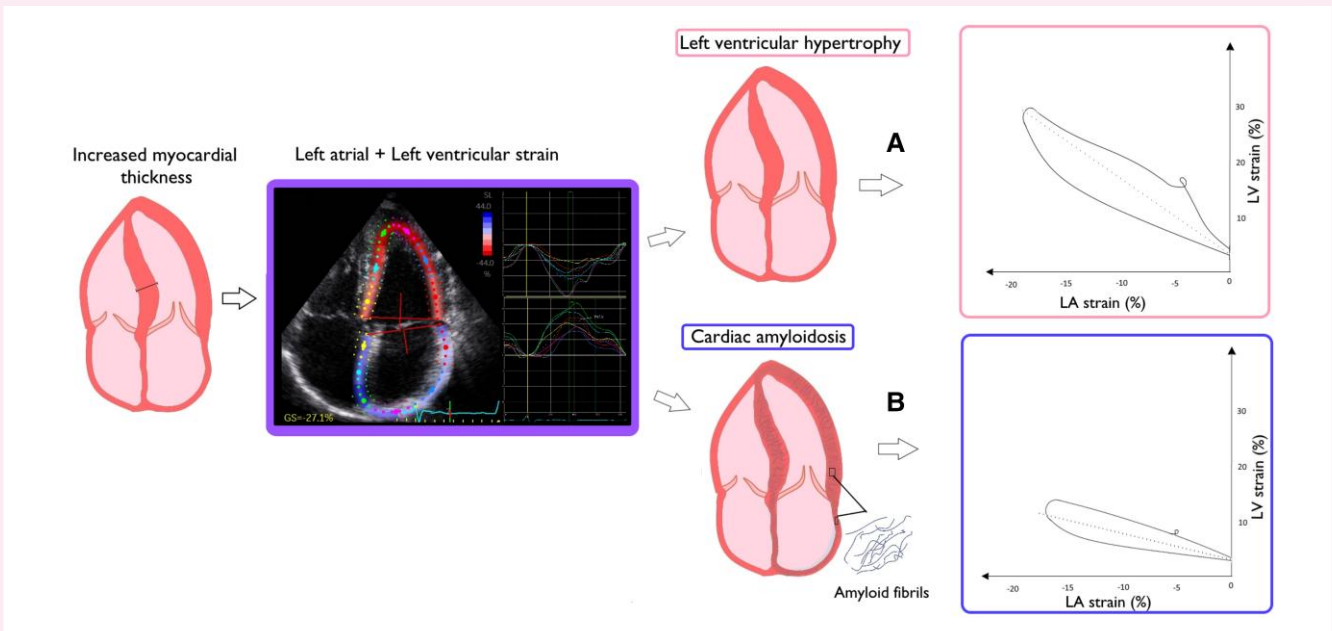

Figure 1 Exemplifying the different strain characteristics with LA–LV strain loop and loop slope of (*A*) true left ventricular hypertrophy and (*B*) cardiac amyloidosis (transthyretin amyloid cardiomyopathy).

Ethics

The study complies with the Declaration of Helsinki and has acquired ethical approval from the regional ethics review board in Umeå, DNR 2016/435-31 M, with supplementary application DNR 2018-418-32 M. All the participants have provided and signed a written informed consent that their information could be used for future research.

Echocardiographic data collection

Echocardiographic examinations were performed on GE Vivid E7, Vivid E9, and Vivid E95 systems (GE Medical Systems, Horten, Norway) equipped with an adult cardiac phased array transducer, 1.5–4.3 MHz. All digitally stored images were acquired in DICOM format using a frame rate of 50–70 frames per second. Analysis and measurements were retrospectively performed offline using GE EchoPAC software version 204 (GE Vingmed Ultrasound AS, USA). LV dimensions estimation such as LV end-diastolic diameter (LVDd), LV end-systolic diameter (LVSd), IVSd, posterior wall thickness (PWT), and relative wall thickness (RWT) calculated as (PWT × 2)/LVDd and LV mass estimation (using the cube formula) were all performed in agreement with echocardiographic guidelines.[28] Diastolic function was assessed through measurements of early (*E*) and late (*A*) peak transmitral wave velocities, and subsequently, *E*/*A* ratio was calculated. Early myocardial tissue (é) velocities were obtained from the septal and lateral LV annulus and averaged to calculate *E*/é. Left atrial volume was measured by the biplane method of discs in apical four- and two-chamber view and indexed (LAVI) to body surface area (BSA). LV ejection fraction (LVEF) was determined using the standardized Simpson biplane method.

Speckle tracking

Strain analysis for determination of LA and LV deformation was derived from B-mode apical four-chamber view images. Speckle tracking and LA–LV strain analyses were measured using EchoPAC (GE) Q-Analysis tracking software.

A rough outline of the LA and LV endocardial borders was manually traced by the expert operator (F.E.) and presented as six segments by the software. If two or more of the segments failed to be recognized by the software in the LA and/or LV, or if apparent chamber foreshortening was present, measurements were considered unreliable and discarded. Tracing data of LV global longitudinal strain (GLS) and LA peak atrial longitudinal strain (PALS) during systole were acquired from the same apical four-chamber image during the same cardiac cycle.

Strain–strain loop

Data from LA–LV strain measurements were exported to create strain loops using Matlab R2022B (MatchWorks Inc, Natik, MA, USA). For each participant, a LA–LV strain loop was reconstructed by plotting the coordinates corresponding to pairs of global LA strain vs. global LV strain from the same segment of the cardiac cycle.[24] LV strain values were set on the *x*-axis and the LA strain values on the *y*-axis. The slope of LV–LA strain loop was estimated through linear regression. Following this, interpolated data were generated between the plotted strain coordinates to compute a finer grid with 0.1% spacing within the loop. An area of the loop was determined by calculating the area under curve (AUC) of the upper part and subtracting AUC of the lower part.

Statistical analyses

SPSS statistics software package (IBM, SPSS version 28) was used to perform all statistical calculations. Unless stated otherwise, continuous variables were expressed as median and interquartile range (IQ) according to distribution and categorical variables as counts and percentages (%). Normality of data was assessed using Shapiro–Wilk test. Comparison of paired data was done with Mann–Whitney *U* test and only between the ATTR-CM and LVH group. Follow-up analyses were done using *post hoc* Mann–Whitney *U* test, and categorical comparisons employed between ATTR-CM and LVH with Fischer's exact test (two-sided). Kruskal–Wallis was applied when comparing median strain values and LA–LV strain loop between all three study groups. A $P < 0.05$ was considered statistically significant. A receiver operating characteristics (ROC) curve analysis was performed to demonstrate the use of the mentioned strain-based functional methods to differentiate ATTR-CM from LVH. DeLong's test was used to evaluate for difference between the ROC curves.

Results

Clinical data

A total of 89 participants that fit the pre-set inclusion criteria were included in the study cohort. One participant within the LVH group was excluded at a late phase due to confirmed AL-amyloidosis. All strain measurements were considered of acceptable quality.

The total study population had a mean age of 68.1 (SD 11.4) years and consisted of 55.1% males. The ATTR-CM group was significantly older than the LVH group ($P = 0.005$). Systolic blood pressure exceeding (SBP) > 140 mmHg or diastolic blood pressure (DBP) exceeding >90 mmHg from one single measurement was recognized in 6 (20.0%) participants within the control group, 12 (41.4%) within ATTR-CM, and 19 (63.3%) in LVH group (see *Table 1*) for clinical characteristics.

Mutations and aetiology

The ATTR-CM group ($n = 30$) included six different ATTRv mutations and six patients with ATTRwt (see *Table 2*). The different main underlying aetiologies for the increased myocardial thickness within the LVH group ($n = 29$) are presented in *Table 3*. Within this group, 13 (44.8%) patients were evaluated with DPD scintigraphy, all with a confirmed negative result for CA (grade 0).

Table 1 Clinical characteristics of the study population

	Healthy control $n = 30$	ATTR-CM $n = 30$	LVH $n = 29$	*P*-value ATTR-CM vs. LVH
Male *n* (%)	14 (46.7)	19 (63.3)	16 (55.2)	0.601
Age	64.0.(12.0)	75.0 (11.5)	71.0 (15.5)	0.005
BSA (m^2)	1.85 (0.29)	1.81 (0.25)	1.99 (0.32)	0.017
Systolic BP (mmHg)	130 (26)	140 (30)	150 (34)	0.022
Diastolic BP (mmHg)	80 (10)	80 (19)	80 (20)	0.421
Heart rate, bpm	68.5 (13.3)	74.0 (17.0)	65.0 (13.3)	0.032

Values are presented as median (interquartile range).
BP, blood pressure; BPM, beats per minute; BSA, body surface area; HR, heart rate.

Table 2 Included transthyretin variants within the transthyretin amyloidosis cardiomyopathy group

Variants	
Val30Met, *n* (%)	19 (63.3)
The60Ala, *n* (%)	1 (3.3)
Val122Ile, *n* (%)	1 (3.3)
Ala45Glys, *n* (%)	1 (3.3)
Ala97Ser, *n* (%)	1 (3.3)
His88Arg, *n* (%)	1 (3.3)
Wild type, *n* (%)	6 (20.0)

Table 3 Included aetiologies in left ventricular hypertrophy group

Aetiology	
Essential hypertension, *n* (%)	10 (34.5)
HCM, *n* (%)	7 (24.1)
Aortic stenosis	
Grade I, *n* (%)	1 (3.4)
Grade II–III, *n* (%)	3 (10.3)
Grade III, *n* (%)	8 (27.6)

Grade I, represents mild stenosis; Grade II, moderate stenosis; and Grade III, severe stenosis.
HCM, hypertrophic cardiomyopathy.

Electrocardiogram

Amongst the ATTR-CM, 10 (33.3%) patients displayed first-degree heart block, 1 (3.3%) individual second-degree heart block, and two (6.7%) with right branch bundle block combined with left fascicular block. In the LVH group, five (17.2%) patients displayed first-degree heart block and one (3.4%) with an incomplete left fascicular block. All control participants were in sinus rhythm.

Myocardial thickness of ATTR-CM vs. LVH

Echocardiographic characteristics are presented in *Table 4*. ATTR-CM participants displayed a significantly more abnormal increase in myocardial thickness when evaluating IVSd, PWT, LV mass, and LV mass/BSA, compared to those in the LVH group (*Table 4*). By estimating LV mass and RWT, all ATTR-CM participants were identified to have concentric LV thickening (RWT > 0.42). In the LVH group, 11 (37.9%) were identified as having concentric hypertrophy and 18 (62.1%) presented with eccentric hypertrophy.

Evaluation of systolic and diastolic function

The total cohort's median LVEF was 59% (IQ 7.5). Patients with ATTR-CM presented with a significantly lower mean LVEF compared to controls ($P = 0.02$). All control participants had an LVEF within normal limits (≥50%).

LV systolic functional assessment showed no significant difference between the two patient groups regarding LV-GLS or LVEF. However, PALS was significantly lower in ATTR-CM compared to LVH ($P = 0.004$) (*Table 4*). Diastolic measurements, including *E*/*A*, E-wave velocities, and *E*/é average, demonstrated no significant difference between ATTR-CM and LVH (*Table 4*). See *Figure 2* for comparison of strain measurements between the three groups.

LA–LV strain loop analysis

All strain analyses combining LA and LV strain values showed significant differences when comparing all three groups ($P < 0.001$). The combined LA–LV strain analyses revealed a significantly lower LA–LV strain slope ($P = 0.014$) and shorter strain loop length ($P = 0.036$) in ATTR-CM group when comparing to the LVH group (*Table 4*). Individual values of LA–LV slopes are presented in *Figure 3*. Examples of LA–LV strain loops from each study group together with strain curves, ECG, and computed slopes are presented in Supplementary data online, *Figures S1–3*. Reproducibility of LA and LV strain has been thoroughly studied previously and proven satisfactory. Other researchers have presented ICC for PALS ranging from 0.80 to 0.97[29] and ICC for LV strain ranging from 0.74 to 0.95.[30]

ROC analysis

ROC analysis was performed to determine the ability for LVEF, PALS, LV-GLS, and LA–LV slope to detect ATTR-CM. The highest AUC was presented for PALS, 0.72. This was comparable to the strain loop slope which displayed an AUC of 0.71 ($P = 0.87$). No significant difference in PALS was demonstrated when comparing the ROC curves to the two methods with lowest AUC, LVEF (63%, $P = 0.22$) and LV-GLS (63%, $P = 0.26$) (*Figure 4*). Comparison was made between the ATTR-CM and LVH groups.

Discussion

The present study explored the significance of LA ATTR amyloid deposits, evaluated with TTE using single and combined simultaneous strain measurements. In our approach, we incorporated both standard strain analysis methods and a novel method using a combined LA–LV strain loop, previously tested in HF patients.[24] To the best of our knowledge, this is the first study using LA–LV strain loop method in patients with CA. We hypothesize that amyloid infiltration of the LA has specific effects on LA function and that this can potentially enable differentiation of CA from other causes of increased myocardial thickness.

Our main findings were as follows: (i) There were significant differences in deformation analysis, especially in PALS and in the LA–LV strain loop characteristics, between the groups ATTR-CM and LVH and (ii) including LA deformation in a combined assessment with LV deformation that can be used in order to present an overview of cardiac performance and clinical follow-up.

Diagnosing ATTR-CM using imaging techniques is complex due to its similarity to other cardiac diseases. Despite advancements in echocardiography, the method still lacks sensitivity to identify specific causes for increased myocardial thickness. Myocardial deformation is considered more sensitive for assessing LV dysfunction in CA than other traditional echocardiographic parameters, such as LVEF.[31] Moreover, in CA, longitudinal systolic function is often significantly reduced early on, while radial and circumferential contractions may remain normal.[17,31]

Amyloid deposition varies, being greater in the basal than in apical segments, leading to base-to-base gradient, or apical-sparring patter, commonly described in CA patients.[32,33] Furthermore, the concentric thickening leaves a relatively small LV cavity. Hence, global measurements, such as LV-GLS and LVEF, do not optimally represent the extent of the LV systolic impairment.

In this study, ATTR-CM showed greater IVSd and LV mass than LVH, but similar left-sided systolic and diastolic function parameters, except for lower PALS seen in ATTR-CM. These results align with previous studies comparing ATTR to other conditions with increased myocardial

Table 4 Echocardiographic characteristics of the study population

Parameters	Healthy control $n = 30$	ATTR-CM $n = 30$	LVH $n = 29$	P-value ATTR-CM vs. LVH
LVDd (mm)	47.0 (6.3)	45.0 (8.3)	48.0 (7.4)	0.003
LVSd (mm)	29.0 (6.3)	31.5 (10.0)	33.0 (10.0)	0.503
IVSD (mm)	10.0 (2.3)	18.0 (5.3)	16.0 (3.5)	0.002
PWT (mm)	8.0 (2.3)	13.5 (3.0)	10.0 (2.0)	<0.001
RWT	0.33 (0.11)	0.59 (0.17)	0.40 (0.11)	<0.001
LV mass (g)	134.3 (57.9)	314.0 (133.8)	270.0 (90.1)	0.013
Indexed LV mass	74.1 (24.5)	172.6 (68.1)	132.6 (30.0)	0.001
E/A	1.0 (0.5)	1.0 (1.0)	0.9 (0.4)	0.237
E-wave (m/s)	0.6 (0.2)	0.7 (0.3)	0.8 (0.4)	0.570
E/é average	8.1 (3.5)	13.8 (5.2)	11.4 (5.5)	0.094
LAVI (cm^3/m^2)	25.5 (9.9)	37.8 (9.9)	38.3 (14.1)	0.214
LVEF (%)	60.0 (3.3)	56.0 (10.3)	59.0 (12.0)	0.096
LV-GLS (%)	−18.2 (4.9)	−14.5 (5.7)	−16.0 (6.0)	0.057*
LA PALS (%)	28.6 (11.3)	12.0 (9.4)	20.5 (9.5)	0.004*
LA–LV strain slope	1.32 (0.56)	0.68 (0.54)	0.95 (0.60)	0.014*
Strain loop length	33.0 (11.2)	19.1 (10.4)	24.3 (9.4)	0.036*

Values are presented as median (interquartile range).
GLS, global longitudinal strain; IVSd, end-diastolic interventricular septum; LAVI, left atrium volume index; LV, left ventricle; LVEF, left ventricular ejection fraction; LVDd, end-diastolic left ventricle dimeter; LVDs, end-systolic left ventricle diameter; PALS, left atrium peak atrium longitudinal strain; PWT, posterior wall thickness; RWT, relative wall thickness.
*P < 0.001 by Kruskal–Wallis when comparing all three groups.

thickness.[10,21] The difference in LA–LV strain loops and PALS indicate greater LA impairment relative to LV dysfunction in ATTR-CM. Since LA function is crucial to heart haemodynamics, assessing the atria during imaging, like TTE and MRI, is essential. Our rationale for assessing LA strain in relation to LV strain was to detect these discrepancies. Mălăscue *et al.*[24] describes an overall strong correlation between LV and LA longitudinal strain function, however with a varying degree during different phases of the cardiac cycle. Discrepancies in LA and LV strain suggest that the atrium may be more sensitive to amyloid infiltration, or amyloid-related HF may present early. Minamisawa *et al.*[34] detected impaired LA strain in V122I gene carriers in sinus rhythm. Their findings also suggest that reduced LA function could reflect early stages of ATTR-CM.

Close interaction between the LA and LV suggests that LA function reflects LV-GLS and filling pressures, with PALS often reduced when LV-GLS is low. Gan *et al.*[35] showed that PALS correlates with LV-GLS and is inversely related to LA volume. In this study, no differences in LAVI were found between ATTR-CM and LVH groups. LA strain, a load-dependant measure, correlates with LV filling pressures and should not be excluded as primary reason for differences in strain results since cardiac amyloidosis is strongly associated with diastolic dysfunction. However, despite similar diastolic measurements (primarily *E/A* and *E/é*), LA dysfunction in ATTR-CM may not be due to LA dilatation but rather intrinsic abnormalities, where amyloid infiltration could be a plausible explanation for causing the LA stiff and non-compliant. Post-mortem biopsies on ATTR-CM patients by Bandera *et al.*[14] showed significant amyloid infiltration and myocyte atrophy, supporting this theory of LA dysfunction.

Clinical implication

As promising therapies for ATTR-CM are rapidly developing, early identification of the disease could significantly affect a patient's clinical outcome. There is demonstrated clinical evidence supporting the evaluation of LA function, as well as a proven distinct association between LA stiffening and the prevalence of atrial electromechanical dissociation and its association with poor prognosis for these patients.[14] Add to this the major risk of developing AF in ATTR-CM and the demonstrated association with LA myocardial dysfunction.[36]

Our results confirm that PAL can detect independent LA dysfunction in ATTR-CM and should be included in echocardiographic assessment of increased myocardial thickness. However, it is important to evaluate echocardiographic parameters in relation to overall cardiac function. Assessing LA function in relative LV function, using LA–LV strain loop slope, offers a better view of global cardiac performance. Including LA strain analysis when suspecting CA raises the possibility of detecting the disease earlier, potentially leading to quicker diagnosis and treatment.

More longitudinal studies should be conducted to further study the consequences of progression of LA dysfunction both for prognostic value and response to treatment. Additionally, assessment of LA dysfunction in relation to the development of AF could help predict those at risk of developing AF and thus help plan interventions and treatment. Furthermore, it would also be of interest to include comparison between subgroup of different ATTR variants in addition to other amyloidosis groups such as AL.

Limitations

This is a retrospective study performed on a small population, overtly due to CA being a rare disease. Results may not reflect the total ATTR-CM population. A limitation with the retrospective design is that the echocardiographic images were not optimized for the specific strain analyses and image quality was lower in the examinations performed with older equipment.

ATTR-CM is commonly associated with an older population, and this is evident in this study. Due to the limited data available on the group with LVH, age was not satisfactorily matched between the patient groups. Additionally, there are known natural age-related changes to LV systolic and diastolic function. Consequently, an older population is more likely to have comorbidities affecting cardiac function such as ischaemic heart disease or diabetes mellitus type II. The effects of such process were not controlled in this study.

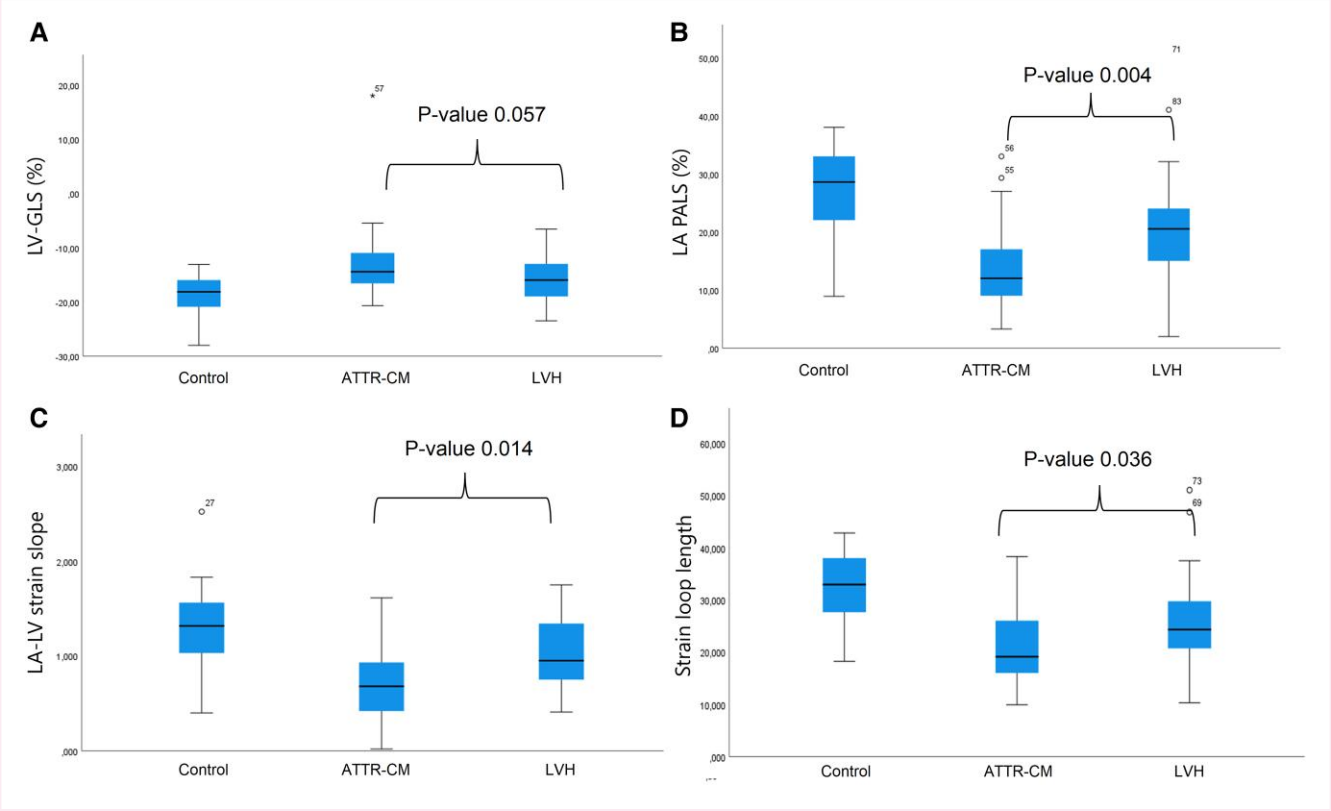

Figure 2 Boxplots demonstrating results for each group regarding (*A*) left ventricle global longitudinal strain (LV-GLS), (*B*) peak atrial longitudinal strain (LA PALS), (*C*) left atrial–left ventricle slope (LA-LV strain slope, and (*D*) strain loop length.

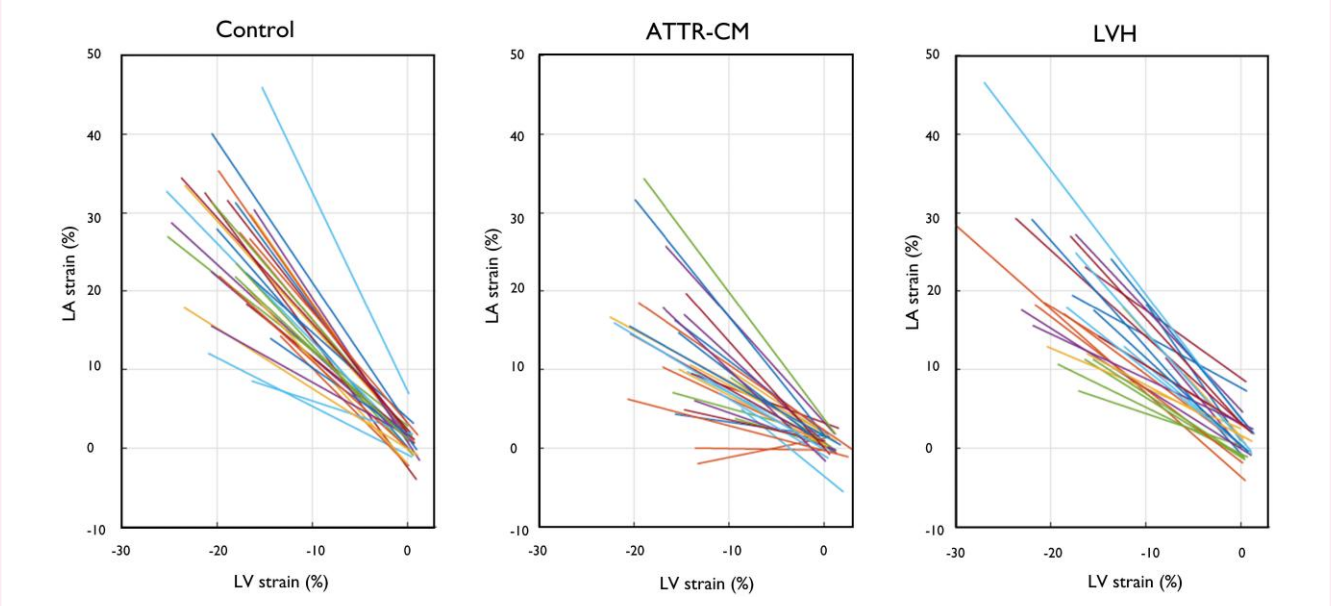

Figure 3 Demonstrating the individual LA–LV slope for each group: control, ATTR-CM, and LVH.

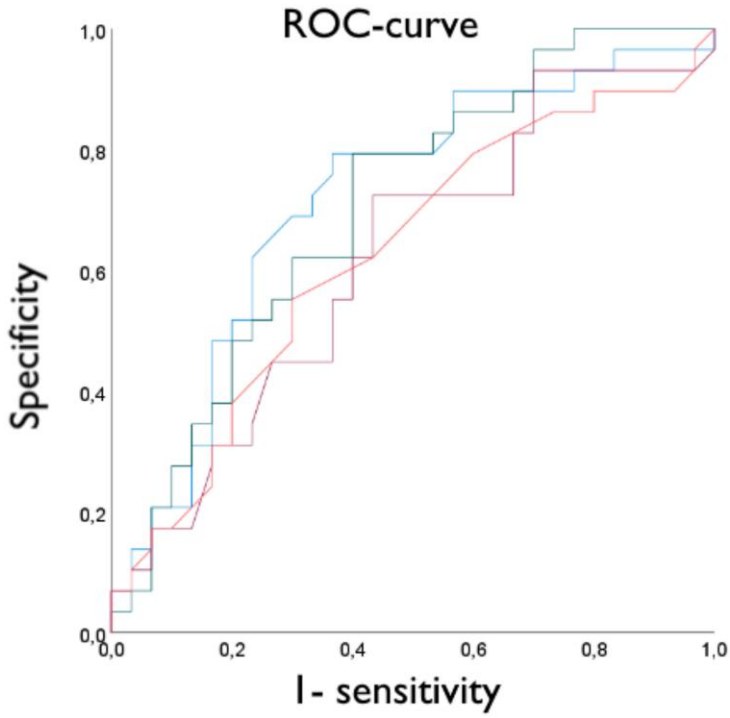

	AUC	95% CI
LVEF	0.63	0.48 - 0.77
LV-GLS	0.62	0.47 - 0.76
LA-PALS	0.72	0.58 - 0.85
LA-LV slope	0.71	0.57 - 0.84

Figure 4 ROC curve demonstrating sensitivity and specificity as well as AUC (CI) for left ventricle ejection fraction, left ventricle global longitudinal strain, left atrial peak atrial longitudinal strain loop length, and left atrial–left ventricular slope.

Some of the images from the study population was acquired as early as 2004, 2006, and 2007 using an older model of GE (Vivid E7). The extent to which this older image processing and quality has on strain analysis using current software is not known, and further prospective deformation studies using strain analysis are advised to be obtained using a recent model only.

Conclusion

We conclude that LA strain was significantly reduced in ATTR-CM compared to LVH. Furthermore, our findings indicate that evaluating LA strain, both independently and in combination with LV-GLS, provides superior diagnostic value in differentiating ATTR-CM from LVH.

The addition of LV strain to LA deformation information displays the mechanical dissociation of the LA in relation to LV in ATTR-CM. This potentially unmasks the effects of atrial amyloid infiltration. Our findings indicate that evaluation of LA strain as a standalone parameter and in combination with LV GLS yield higher sensitivity and specificity than LV-GLS alone and strengthen any suspicion of intrinsic atrial dysfunction in ATTR-CM that is less likely to be found in other pathologies causing LVH. We found this result to agree with prior understanding of atrial function and effects of amyloid engagement and highlight the value of including LA deformation analysis in clinical evaluations.

Supplementary data

Supplementary data are available at *European Heart Journal - Imaging Methods and Practice* online.

Funding

This study was funded by the Swedish research council (2019-01338 and 2022-01254) and Swedish Heart and Lung Foundation (20200160).

Conflict of interest: P.L. is a consulting lecturer and a member of advisory board of Pfizer.

Data availability

The data underlying this article cannot be shared publicly due to the privacy regulations and requirements of authorities. The data will be shared on reasonable request to the corresponding author.

Lead author biography

Fredrik Edbom is a Swedish biomedical scientist in clinical physiology with main experience in ultrasound imaging. He is currently a PhD candidate at the Umeå University Hospital with research interest in echocardiography surrounding heart failure and cardiac amyloidosis.

References

1. Donnelly JP, Hanna M. Cardiac amyloidosis: an update on diagnosis and treatment. *Cleve Clin J Med* 2017;**84**:12–26.
2. Siddiqi OK, Ruberg FL. Cardiac amyloidosis: an update on pathophysiology, diagnosis, and treatment. *Trends Cardiovasc Med* 2018;**28**:10–21.
3. Oghina S, Bougouin W, Bezard M, Kharoubi M, Komajda M, Cohen-Solal A *et al.* The impact of patients with cardiac amyloidosis in HFpEF trials. *JACC Heart Fail* 2021;**9**:169–78.
4. Muchtar E, Dispenzieri A, Magen H, Grogan M, Mauermann M, McPhail ED *et al.* Systemic amyloidosis from A (AA) to T (ATTR): a review. *J Intern Med* 2021;**289**:268–92.
5. Ruberg FL, Grogan M, Hanna M, Kelly JW, Maurer MS. Transthyretin amyloid cardiomyopathy: JACC state-of-the-art review. *J Am Coll Cardiol* 2019;**73**:2872–91.
6. AbouEzzeddine OF, Davies DR, Scott CG, Fayyaz AU, Askew JW, McKie PM *et al.* Prevalence of transthyretin amyloid cardiomyopathy in heart failure with preserved ejection fraction. *JAMA Cardiol* 2021;**6**:1267–74.
7. Mohammed SF, Mirzoyev SA, Edwards WD, Dogan A, Grogan DR, Dunlay SM *et al.* Left ventricular amyloid deposition in patients with heart failure and preserved ejection fraction. *JACC Heart Fail* 2014;**2**:113–22.
8. Steiner I, Hajkova P. Patterns of isolated atrial amyloid: a study of 100 hearts on autopsy. *Cardiovasc Pathol* 2006;**15**:287–90.
9. Porcari A, Bussani R, Merlo M, Varra GG, Pagura L, Rozze D *et al.* Incidence and characterization of concealed cardiac amyloidosis among unselected elderly patients undergoing post-mortem examination. *Front Cardiovasc Med* 2021;**8**:749523.
10. Rausch K, Scalia GM, Sato K, Edwards N, Lam AK, Platts DG *et al.* Left atrial strain imaging differentiates cardiac amyloidosis and hypertensive heart disease. *Int J Cardiovasc Imaging* 2021;**37**:81–90.
11. Nochioka K, Quarta CC, Claggett B, Roca GQ, Rapezzi C, Falk RH *et al.* Left atrial structure and function in cardiac amyloidosis. *Eur Heart J Cardiovasc Imaging* 2017;**18**:1128–37.
12. Benjamin MM, Arora P, Munir MS, Darki A, Liebo M, Yu M *et al.* Association of left atrial hemodynamics by magnetic resonance imaging with long-term outcomes in patients with cardiac amyloidosis. *J Magn Reson Imaging* 2023;**57**:1275–84.
13. Papathanasiou M, Jakstaite AM, Oubari S, Siebermair J, Wakili R, Hoffmann J *et al.* Clinical features and predictors of atrial fibrillation in patients with light-chain or transthyretin cardiac amyloidosis. *ESC Heart Fail* 2022;**9**:1740–8.
14. Bandera F, Martone R, Chacko L, Ganesananthan S, Gilbertson JA, Ponticos M *et al.* Clinical importance of left atrial infiltration in cardiac transthyretin amyloidosis. *JACC Cardiovasc Imaging* 2022;**15**:17–29.
15. de Gregorio C, Dattilo G, Casale M, Terrizzi A, Donato R, Di Bella G. Left atrial morphology, size and function in patients with transthyretin cardiac amyloidosis and primary hypertrophic cardiomyopathy—comparative strain imaging study. *Circ J* 2016;**80**:1830–7.
16. Bisbal F, Baranchuk A, Braunwald E, Bayes de Luna A, Bayes-Genis A. Atrial failure as a clinical entity: JACC review topic of the week. *J Am Coll Cardiol* 2020;**75**:222–32.
17. Falk RH, Quarta CC. Echocardiography in cardiac amyloidosis. *Heart Fail Rev* 2015;**20**:125–31.
18. Jin FQ, Kakkad V, Bradway DP, LeFevre M, Kisslo J, Khouri MG *et al.* Evaluation of myocardial stiffness in cardiac amyloidosis using acoustic radiation force impulse and natural shear wave imaging. *Ultrasound Med Biol* 2023;**49**:1719–27.
19. Palmiero G, Rubino M, Monda E, Caiazza M, D'Urso L, Carlomagno G *et al.* Global left ventricular myocardial work efficiency in heart failure patients with cardiac amyloidosis: pathophysiological implications and role in differential diagnosis. *J Cardiovasc Echogr* 2021;**31**:157–64.
20. de Gregorio C, Trimarchi G, Faro DC, De Gaetano F, Campisi M, Losi V *et al.* Myocardial work appraisal in transthyretin cardiac amyloidosis and nonobstructive hypertrophic cardiomyopathy. *Am J Cardiol* 2023;**208**:173–9.
21. Aimo A, Fabiani I, Giannoni A, Mandoli GE, Pastore MC, Vergaro G *et al.* Multi-chamber speckle tracking imaging and diagnostic value of left atrial strain in cardiac amyloidosis. *Eur Heart J Cardiovasc Imaging* 2022;**24**:130–41.
22. Usuku H, Takashio S, Yamamoto E, Yamada T, Egashira K, Morioka M *et al.* Prognostic value of right ventricular global longitudinal strain in transthyretin amyloid cardiomyopathy. *J Cardiol* 2022;**80**:56–63.
23. Vergaro G, Aimo A, Rapezzi C, Castiglione V, Fabiani I, Pucci A *et al.* Atrial amyloidosis: mechanisms and clinical manifestations. *Eur J Heart Fail* 2022;**24**:2019–28.
24. Malaescu GG, Mirea O, Capota R, Petrescu AM, Duchenne J, Voigt JU. Left atrial strain determinants during the cardiac phases. *JACC Cardiovasc Imaging* 2022;**15**:381–91.
25. Garcia-Pavia P, Kristen AV, Drachman B, Carlsson M, Amass L, Angeli FS *et al.* Survival in a real-world cohort of patients with transthyretin amyloid cardiomyopathy treated with tafamidis: an analysis from the transthyretin amyloidosis outcomes survey (THAOS). *J Card Fail* 2024:S1071-9164(24)00222-7. https://doi.org/10.1016/j.cardfail.2024.06.003
26. Elliott P, Drachman BM, Gottlieb SS, Hoffman JE, Hummel SL, Lenihan DJ *et al.* Long-Term survival with tafamidis in patients with transthyretin amyloid cardiomyopathy. *Circ Heart Fail* 2022;**15**:e008193.
27. Lindqvist P, Waldenstrom A, Henein M, Morner S, Kazzam E. Regional and global right ventricular function in healthy individuals aged 20–90 years: a pulsed Doppler tissue imaging study: Umea General Population Heart Study. *Echocardiography* 2005;**22**:305–14.
28. Lang RM, Badano LP, Mor-Avi V, Afilalo J, Armstrong A, Ernande L *et al.* Recommendations for cardiac chamber quantification by echocardiography in adults: an update from the American Society of Echocardiography and the European Association of Cardiovascular Imaging. *J Am Soc Echocardiogr* 2015;**28**:1–39 e14.
29. Mandoli GE, Pastore MC, Procopio MC, Pica A, Vigna M, Benfari G *et al.* Unveiling the reliability of left atrial strain measurement: a dedicated speckle tracking software perspective in controls and cases. *Eur Heart J Imaging Methods Pract* 2024;**2**:qyae061.
30. Karlsen S, Dahlslett T, Grenne B, Sjoli B, Smiseth O, Edvardsen T *et al.* Global longitudinal strain is a more reproducible measure of left ventricular function than ejection fraction regardless of echocardiographic training. *Cardiovasc Ultrasound* 2019;**17**:18.
31. Quarta CC, Solomon SD, Uraizee I, Kruger J, Longhi S, Ferlito M *et al.* Left ventricular structure and function in transthyretin-related versus light-chain cardiac amyloidosis. *Circulation* 2014;**129**:1840–9.
32. Phelan D, Collier P, Thavendiranathan P, Popovic ZB, Hanna M, Plana JC *et al.* Relative apical sparing of longitudinal strain using two-dimensional speckle-tracking echocardiography is both sensitive and specific for the diagnosis of cardiac amyloidosis. *Heart* 2012;**98**:1442–8.
33. Arnberg E, Eldhagen P, Lofbacka V, Venkateshvaran A, Pilebro B, Lindqvist P. RWT/SaVR-A simple and highly accurate measure screening for transthyretin cardiac amyloidosis. *J Clin Med* 2022;**11**:4120.
34. Minamisawa M, Inciardi RM, Claggett B, Cuddy SAM, Quarta CC, Shah AM *et al.* Left atrial structure and function of the amyloidogenic V122I transthyretin variant in elderly African Americans. *Eur J Heart Fail* 2021;**23**:1290–5.
35. Gan GCH, Bhat A, Chen HHL, Fernandez F, Byth K, Eshoo S *et al.* Determinants of LA reservoir strain: independent effects of LA volume and LV global longitudinal strain. *Echocardiography* 2020;**37**:2018–28.
36. Henein MY, Suhr OB, Arvidsson S, Pilebro B, Westermark P, Hornsten R *et al.* Reduced left atrial myocardial deformation irrespective of cavity size: a potential cause for atrial arrhythmia in hereditary transthyretin amyloidosis. *Amyloid* 2018;**25**:46–53.